

Interpolation methods for the kernel of f-k migration

Zaiming Jiang and John C. Bancroft

ABSTRACT

The theory of f-k migration tells us that migration of a stacked seismic section in time-space domain can be done by a mapping operation in frequency-wavenumber domain. The mapping operation involves interpolation among samples of the discrete Fourier transform of the stacked section. This process introduces artifacts into the migrated section. In fact, crude interpolation is the main source of artifacts in f-k migration. The first refined interpolation method, the complex sinc method, was introduced in 1981. Another one, Muir's method, was discussed in 1997. There is an implementation of complex sinc interpolation in the CREWES educational software and data release (MATLAB).

This report discusses interpolation methods and related artifacts. The details of implementing complex sinc interpolation and Muir's interpolation include changing the interpolation formulas according to the Fast Fourier Transform algorithm used, employing mathematical limits of functions to prevent computational overflow, and taking periodic boundary extension instead of zero-padding. It is shown that the two interpolation methods perform almost the same in the sense of both migration quality and computational cost.

INTRODUCTION

Presenting the general exploding reflectors model wavefield as

$$\psi(x, z, t) = \int \int_{-\infty}^{\infty} \varphi(k_x, f) e^{2\pi i(ft - k_x x + k_z z)} dk_x df, \quad (1)$$

where

$$k_z = \sqrt{\frac{f^2}{v^2} - k_x^2}, \quad (2)$$

the stacked section and the migrated section can be denoted as

$$\begin{aligned} \psi(x, z=0, t) &= \int \int_{-\infty}^{\infty} \varphi(k_x, f) e^{2\pi i(ft - k_x x)} dk_x df, \\ \psi(x, z, t=0) &= \int \int_{-\infty}^{\infty} \theta(k_x, k_z) e^{2\pi i(k_z z - k_x x)} dk_x dk_z, \end{aligned} \quad (3)$$

where

$$\theta(k_x, k_z) = \frac{vk_z}{\sqrt{k_x^2 + k_z^2}} \varphi(k_x, v\sqrt{k_x^2 + k_z^2}). \quad (4)$$

Since $\varphi(k_x, f)$ and $\theta(k_x, k_z)$ can be identified as the 2D Fourier transform of the stacked section and the migrated section, migration from the stacked section in time-space

domain becomes mapping from $\varphi(k_x, f)$ to $\theta(k_x, k_z)$ in frequency-wavenumber domain. This is the principle of f-k migration.

Mapping from $\varphi(k_x, f)$ to $\theta(k_x, k_z)$ in the frequency-wavenumber domain involves interpolation among the discrete samples of $\varphi(k_x, f)$. There are many interpolation methods. People regard complex sinc interpolation as the best method. Complex sinc interpolation was first introduced by Rosenbaum in 1981. Then the next year Harlan gave a truncated version of the method, which employs 10 samples to interpolate. Persons in the SEP (Lin et al., 1997, Blondel et al., 1997, and Popovici et al., 1997) discussed another refined interpolation method, which is called by Lin "Muir's interpolation".

There is an implementation of complex sinc interpolation in the CREWES educational software and data release (MATLAB) (Margrave, 2003). It is due to Harlan's design, but it employs an arbitrary even number (default number is 8) of samples to interpolate. There are also other interpolation functions in the software, such as nearest neighbor interpolation, spline interpolation, and complex linear interpolation.

The following sections discuss interpolation related artifacts and the implementation of complex sinc interpolation and Muir's interpolation based on Bancroft's f-k migration software.

INTERPOLATION ARTIFACTS

A model, MODEL50.SGY, is used as the stacked section (Figure 1). There are 150 traces and 750 samples in each trace in the model. After Fourier transform, there are 256 traces and 1024 samples in each trace.

There are eight dips, two spikes, two diffractions, and a horizontal reflector in the stacked section. These reflectors are expected to be migrated to eight dips with greater angles, two upturned semi-circles (from the two spikes), two spikes (from the two diffractions), and a horizontal reflector.

In addition, upturned semi-circles are expected to be present at the ends of terminating reflectors in the migrated section because the model does not perfectly portray the terminating reflectors. A terminating reflector in a CMP stack section should show diffractions at the ends (Figure 2). The branch under the reflector is called the backward branch, and the other side is called the forward branch. The pulses on the reflector and the forward branch of the diffraction have the same polarity, but the pulses on the backward branch of the diffraction have the opposite polarity. The model does not model the diffractions at the ends of terminating reflectors. Hence, upturned semi-circles are expected to be present at the ends of the reflectors in the migrated section, and the two branches have different pulse polarities. On one hand, the upturned semi-circles present at the ends of the reflectors are not regarded as artifacts; on the other hand, if the upturned semi-circles are not present or weakly present, or downturned curves are present, they are regarded as artifacts.

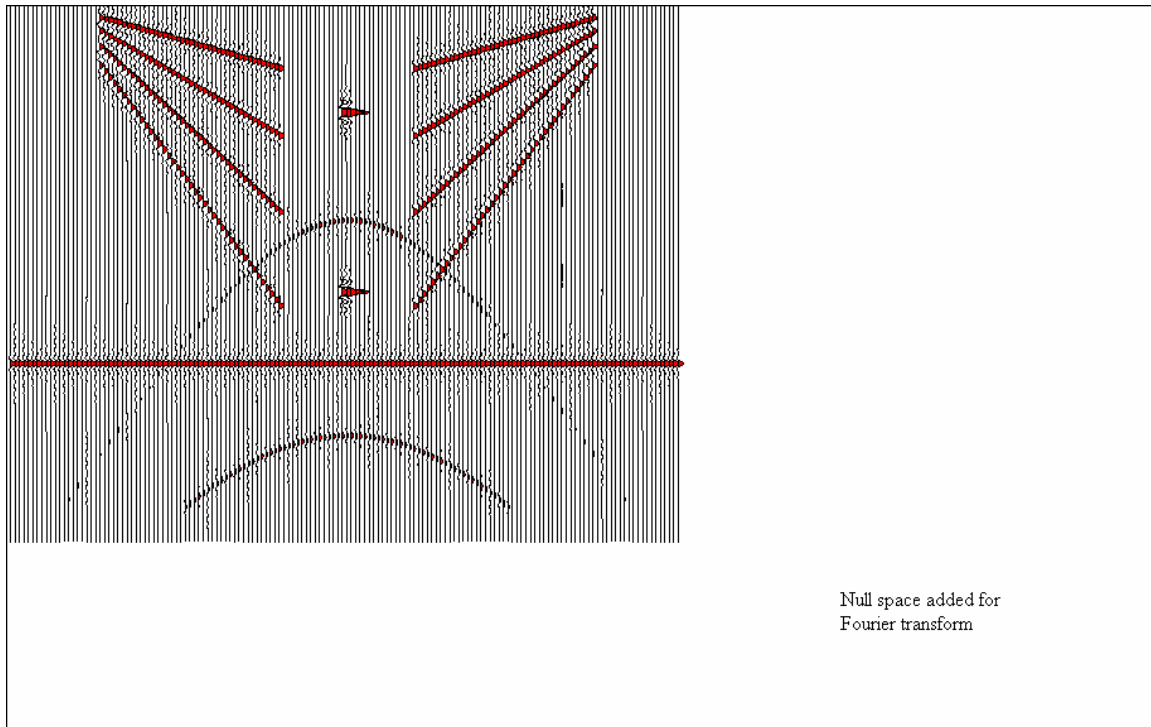


FIG. 1. Model of stacked section. It has a seismic data set of 150 traces and 750 samples in each trace. However, it is shown as 256 traces and 1024 samples in each trace for the sake of comparison with the migrated sections, which have 256 traces and 1024 samples in each trace.

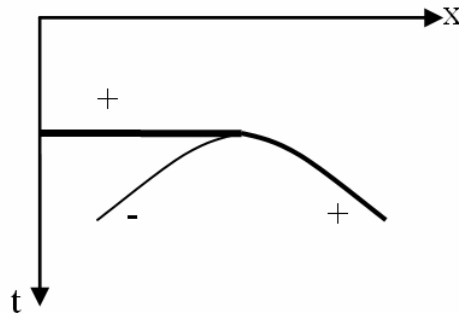


FIG. 2. A terminating reflector in a CMP stack section should show diffractions. The reflector and the forward branch have the same pulse polarity, the backward branch have the opposite pulse polarity. (Adapted from Krebs, 2006)

Bancroft uses truncation interpolation, linear interpolation, and complex linear interpolation in his f-k migration software.

Truncation interpolation is the simplest method. It just uses a close sample value as the interpolated value. This method results in a lot of artifacts in the migrated section (Figure 3). The artifacts include: (1) the dark lines parallel to the dips. They are shown all over the section. (2) The downturned curves connected to the spikes and upturned semi-circles. (3) The downturned curves and upturned semi-circles at the ends of the terminating reflectors. The later are regarded as artifacts because they are too weak.

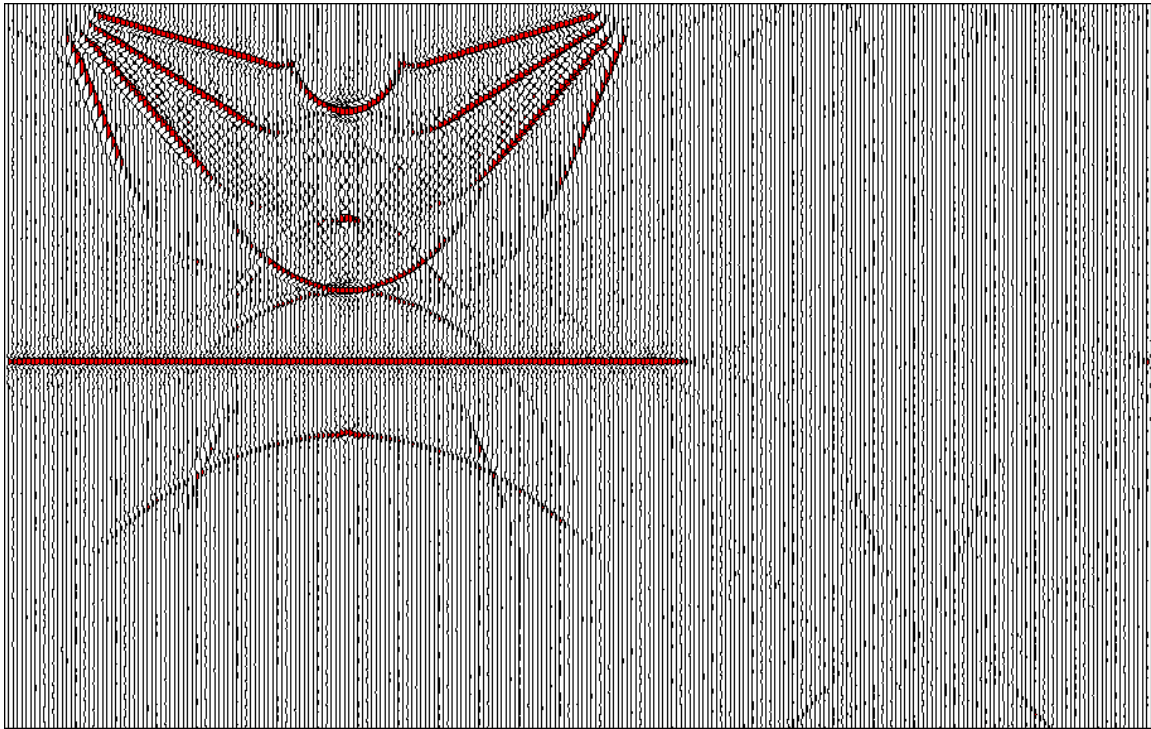


FIG. 3. Migrated section resulted from the truncation interpolation method. Straight dark lines parallel to the dips, downturned curves connected to the spikes and the upturned semi-circles, and weak curves at the ends of the terminating reflectors are artifacts.

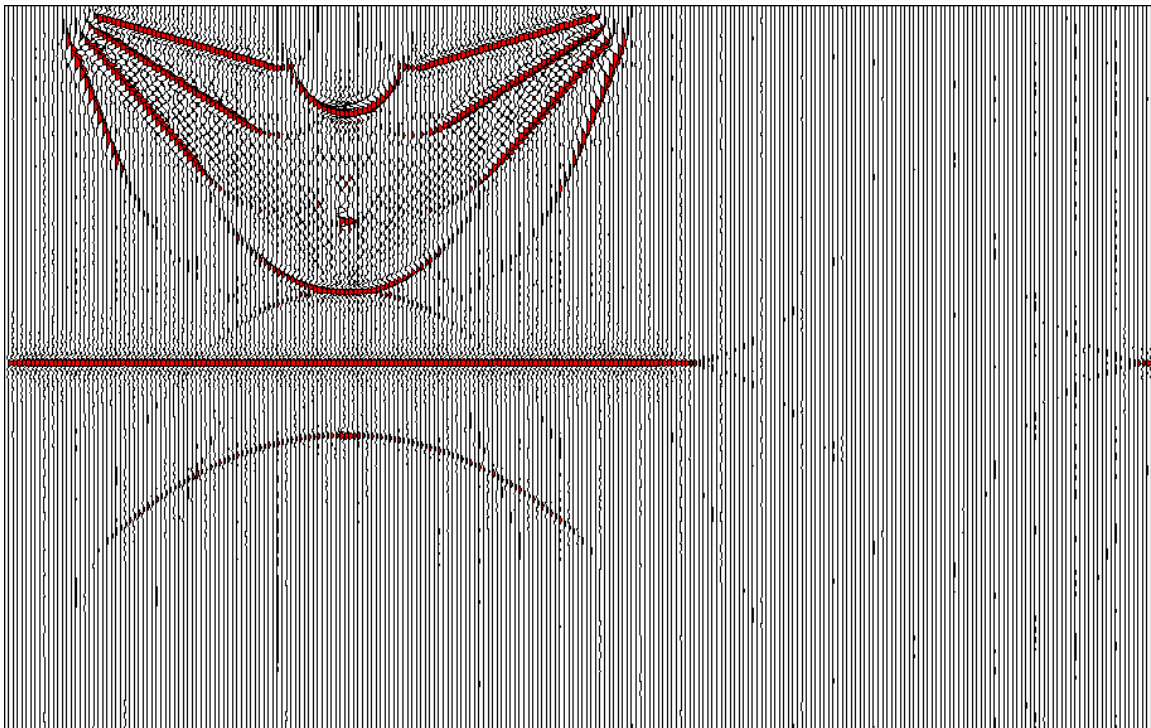


FIG. 4. Migrated section resulting from the linear interpolation method. Downturned curves connected to the spikes and the upturned semi-circles, and weak curves at the ends of the terminating reflectors are artifacts.

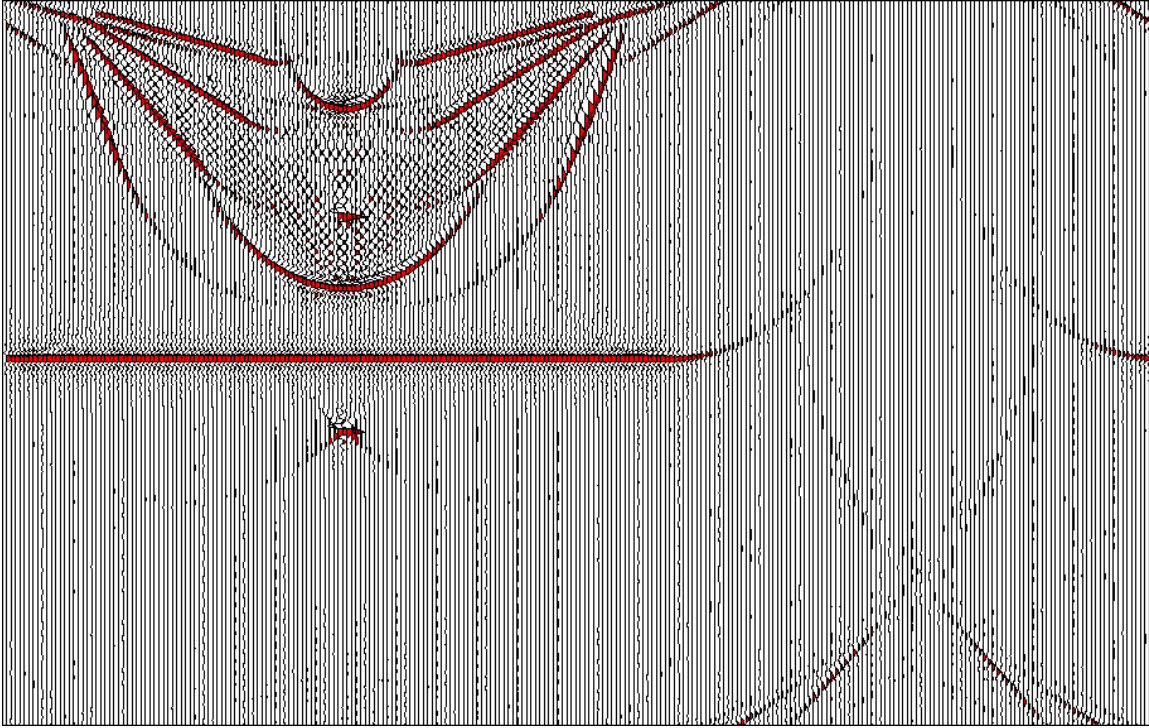


FIG. 5. Migrated section resulted from complex linear interpolation method. The dark lines parallel to the dips are artifacts.

The linear interpolation method results in a better migrated section. However, a lot of artifacts are still present (Figure 4). The artifacts are similar to the ones from truncation interpolation, except that the dark lines parallel to the dips are weaker.

Complex linear interpolation is basically linear interpolation with phase shift operators. The most significant artifacts are the dark lines parallel to the dips (Figure 5).

COMPLEX SINC INTERPOLATION

Using the following forward and backward Fourier transform pair,

$$\begin{aligned} X(f) &= \int_{-\infty}^{\infty} x(t)e^{-i2\pi ft} dt \\ x(t) &= \int_{-\infty}^{\infty} X(f)e^{i2\pi ft} df \end{aligned} \quad (5)$$

the complex sinc interpolation formula is

$$\varphi_r = \sum_{n=0}^{N-1} \varphi_n e^{-i[(r-n)\pi]} \frac{\sin[(r-n)\pi]}{(r-n)\pi}. \quad (6)$$

This formula can also be denoted as a convolution in the frequency domain,

$$\varphi_r = \left[\sum_{n=0}^{N-1} \varphi_n \delta(r-n) \right] * [\text{sinc}(r) e^{-ir\pi}]. \quad (7)$$

Recognizing that the normalized sinc function in the frequency domain is a rectangular pulse i.e., a box-car filter, in the time domain, and that the phase shift operator $e^{-ir\pi}$ delays the box-car by half of the time period, the complex sinc interpolation formula can be interpreted as using a box-car filter in the time domain from $t=0$ to $t=t_{max}$ to “eliminate” the periodic representations other than the primary time period.

There are three tricky points in the implementation of complex sinc interpolation.

The first one pertains to the sign in the exponential of the Fourier transform.

When people use the forward and backward Fourier transform pair denoted in equation 5, the complex sinc interpolation formula is equation 6. However, in our work environment, the existing FFT (Fast Fourier Transform) and the IFFT (Inverse FFT) employ different signs in the exponential part, i.e., the Fourier transform pair is

$$\begin{aligned} X(f) &= \int_{-\infty}^{\infty} x(t) e^{i2\pi ft} dt \\ x(t) &= \int_{-\infty}^{\infty} X(f) e^{-i2\pi ft} df \end{aligned} \quad (8)$$

Under this condition, the complex sinc interpolation formula used in the program needs a sign change for the exponential part, too. Thus,

$$\varphi_r = \sum_{n=0}^{N-1} \varphi_n e^{+i[(r-n)\pi]} \frac{\sin[(r-n)\pi]}{(r-n)\pi}. \quad (9)$$

The second tricky point is about preventing numerical overflow. Directly calculating $F_n e^{i[(r-n)\pi]} \frac{\sin[(r-n)\pi]}{(r-n)\pi}$ might result in overflow because the denominator, $(r-n)\pi$, might be very small. To prevent overflow, we need to employ the following limit,

$$\lim_{r \rightarrow n} \frac{\sin[(r-n)\pi]}{(r-n)\pi} = 1. \quad (10)$$

The third trick deals with using periodic extension at the boundary instead of a zero-padding scheme. Periodic boundary extension means that when interpolating close to the boundary of the data, computation is performed as if the data is periodically extended. The reason of taking periodic boundary extension is that the spectrum in the frequency domain is periodic. By choosing the periodic extension scheme, the quality of the migrated sections is slightly improved.

The complex sinc function uses all the samples in line to interpolate. However, one can choose part of the samples in line to get a cursory result with less computational effort. Our program is designed to use a variable length of samples to interpolate. The

result of using all the 1024 samples in interpolation is shown in Figure 6. The results of using other different lengths of samples in interpolation are shown in Figure 7.

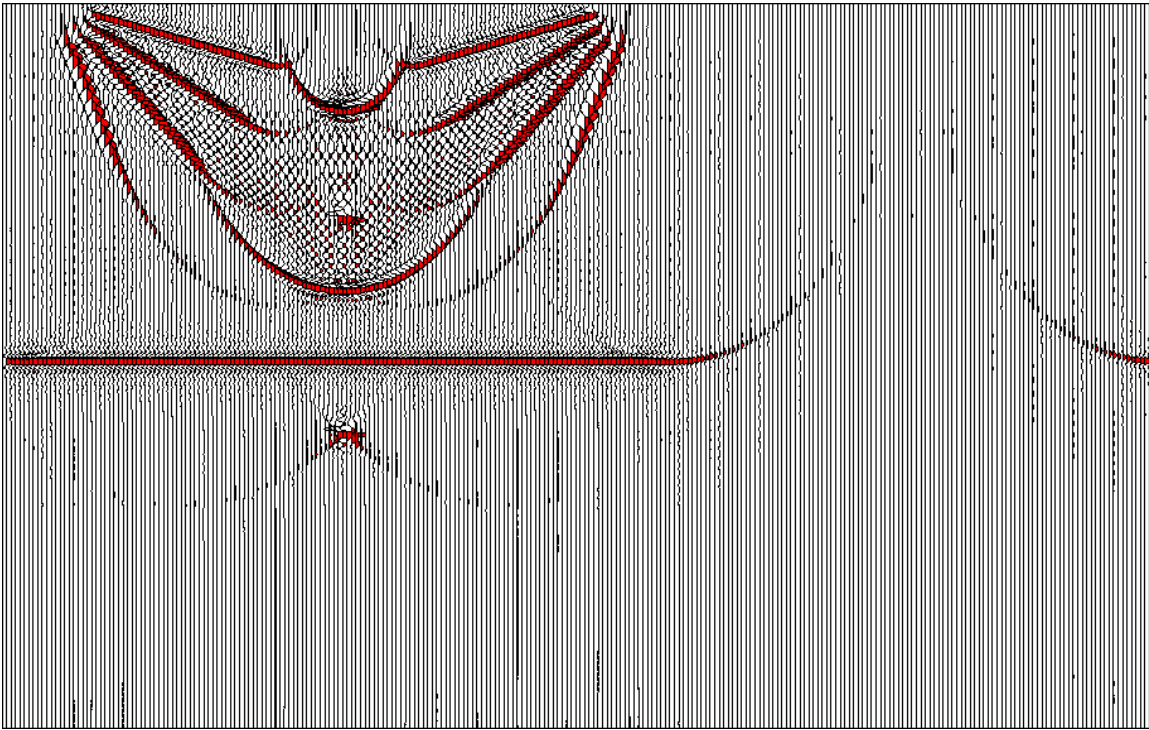


FIG. 6. Migrated section resulted from complex sinc interpolation method. This is the result of using all the 1024 samples in line to interpolate. Artifacts are significantly attenuated.

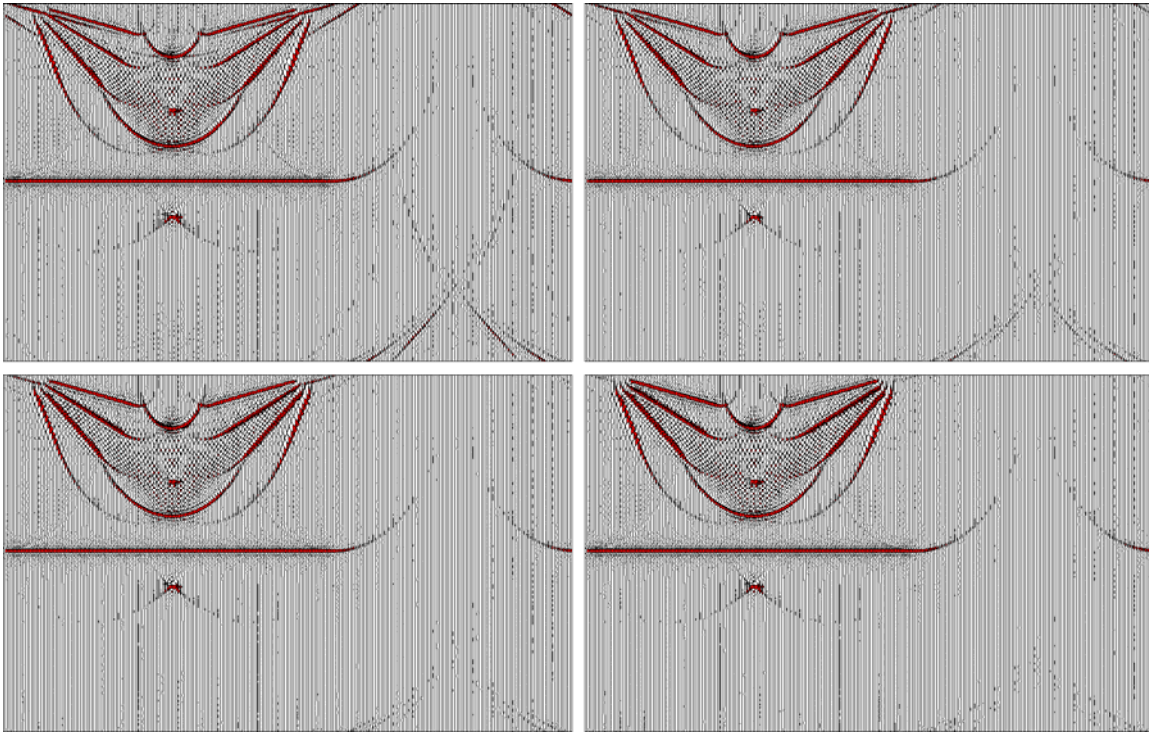


FIG. 7. Migrated sections resulted from complex sinc interpolation method. These are the results of using two (top-left), four (top-right), eight (bottom-left) and sixteen (bottom-right) samples in line to interpolate. Artifacts are gradually attenuated when the number of samples used in interpolation increases.

It can be observed that, (1) the interpolation related artifacts are significantly attenuated by using complex sinc interpolation method; (2) The more the samples are used in interpolation, the more the artifacts are attenuated.

MUIR'S INTERPOLATION

Spectrum φ_r at a continuous frequency r can be denoted by continuous Fourier transform (CFT, some people call it Slow Fourier transform) of the a discrete, evenly sampled N length time function f_n , which, in turn, can be denoted by the inverse discrete Fourier transform of discrete spectrum φ_n . Thus, Muir's interpolation formula is derived as following:

$$\begin{aligned} \varphi_r &= [\text{CFT}](f_n) = \sum_{k=0}^{N-1} f_k e^{-2\pi \frac{rk}{N}} = \sum_{k=0}^{N-1} \{[\text{IDFT}](\varphi_n)\} e^{-2\pi \frac{rk}{N}} \\ &= \sum_{k=0}^{N-1} \left[\frac{1}{N} \sum_{m=0}^{N-1} \varphi_m e^{2\pi \frac{mk}{N}} \right] e^{-2\pi \frac{rk}{N}} = \frac{1}{N} \sum_{m=0}^{N-1} \varphi_m e^{-i(r-m)(1-\frac{1}{N})\pi} \frac{\sin[\pi(r-m)]}{\sin[\pi \frac{(r-m)}{N}]} \end{aligned} \quad (11)$$

When $N \rightarrow \infty$, the formula becomes identical to the complex sinc interpolation.

The implementation of Muir's interpolation method involves the same tricks as complex sinc interpolation, including using opposite sign in the exponential part,

preventing numerical overflow, and taking periodic extension at the boundary instead of zero-padding. The difference is that to prevent overflow, the following limit is used,

$$\lim_{r \rightarrow m} \frac{\sin[\pi(r-m)]}{\sin[\pi \frac{(r-m)}{N}]} = N. \quad (12)$$

Similar to the complex sinc interpolation, the program of Muir's interpolation is designed to use a variable length of samples to interpolate. The result of using all the 1024 samples in line in interpolation is shown in Figure 8. The results of using other different lengths of samples in interpolation are shown in Figure 9.

It can be observed that the results of Muir's interpolation are almost the same as those of complex sinc interpolation.

The computational costs of f-k migration using Muir's interpolation formula, and complex sinc interpolation formula, are shown in Figure 10. The computational costs of the two methods are comparable.

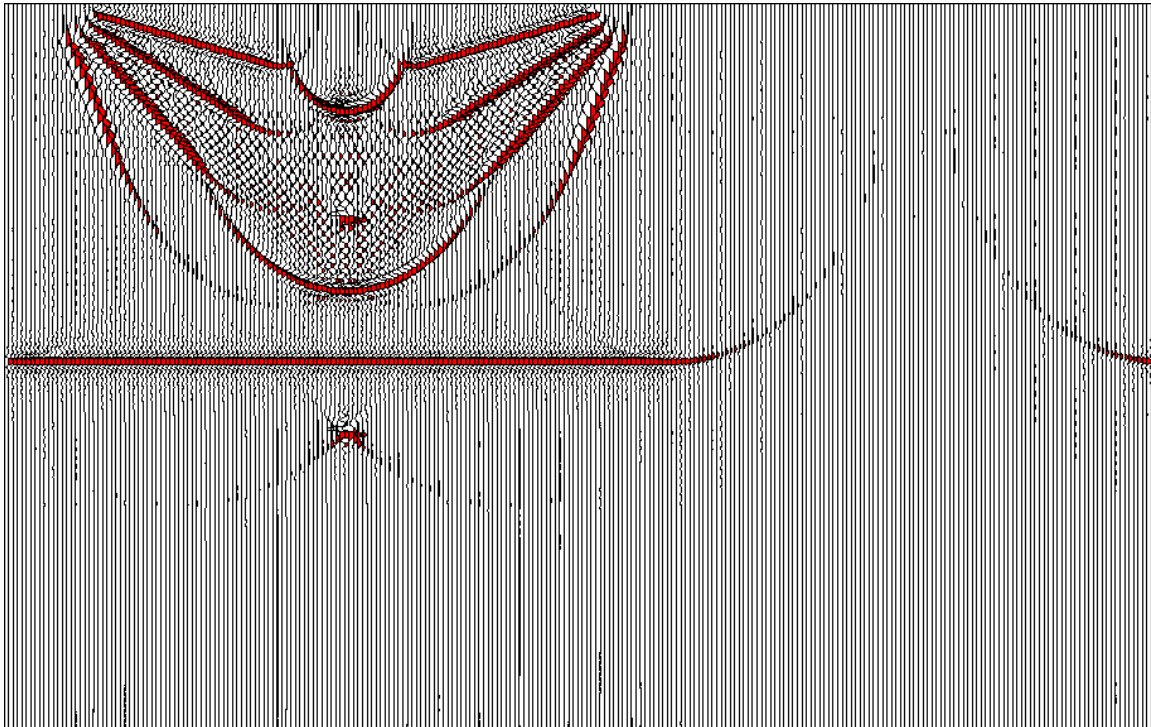


FIG. 8. Migrated section resulted from Muir's interpolation method. This is the result of using all the 1024 samples in line to interpolate. The result is similar to that of complex sinc interpolation.

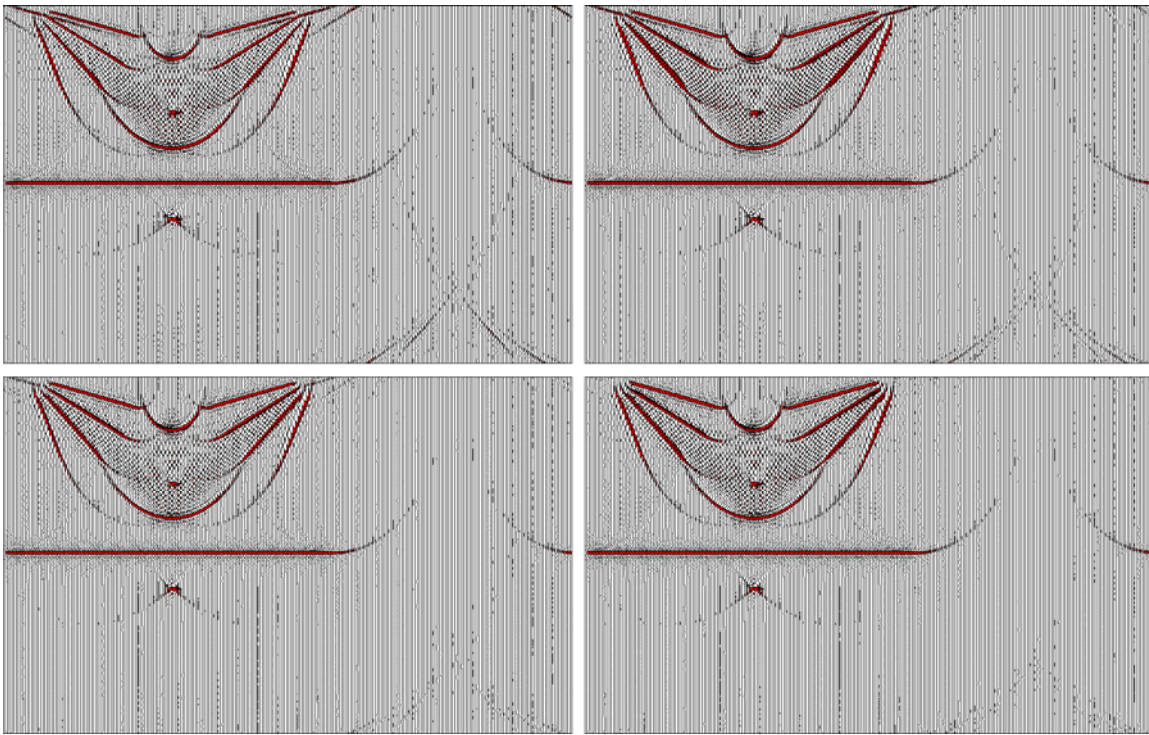


FIG. 9. Migrated sections resulted from Muir's interpolation method. These are the results of using two (top-left), four (top-right), eight (bottom-left) and sixteen (bottom-right) samples in line to interpolate. The results are similar to those of complex sinc interpolation.

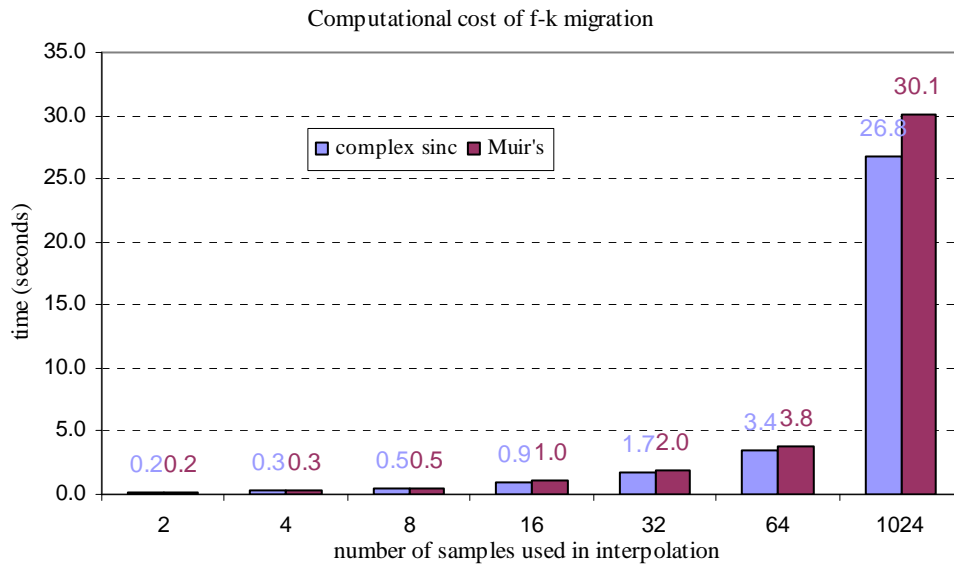


FIG. 10. Computational costs of f-k migration using complex sinc interpolation and Muir's interpolation. The costs of the two interpolation methods are comparable.

CONCLUSIONS

Interpolation in the f-k space introduces artifacts into the migrated section.

When a synthetic model is used as the stacked section, the imperfections in the model, such as the effect of terminating reflectors, should be verified from artifacts.

Designation of complex sinc interpolation and Muir's interpolation involves the tricky points of using appropriate sign in the exponential part according to the FFT arithmetic used, preventing numerical overflow by employing limits of functions, and taking periodic extension at the boundary instead of zero-padding.

By applying complex sinc or Muir's interpolation method, artifacts are attenuated. The more samples used in interpolation, the more the artifacts are attenuated. Interpolating with 8~12 samples results in reasonable migrated sections.

Muir's interpolation method performs almost the same as complex sinc interpolation in the sense of both migration quality and computational cost.

ACKNOWLEDGEMENTS

We would like to thank Gary F. Margrave for his suggestion on boundary extension scheme of interpolation. The discussions with Yongwang Ma and Zimin Zhang are helpful. We also received assistance from a number of other CREWES personal.

We are grateful for the financial support of the CREWES sponsors. We also thank GEDCO for providing access to VISTA, which is used for displaying seismic data in this report.

REFERENCES

- Bancroft, J.C., 2006, A practical understanding of pre- and poststack migration, Course notes.
- Blondel, P. and Muir, F., 1997, Parallel computing exhumed slow Fourier transform in Stolt migration: SEP-79, 279-287.
- Harlan, W., 1982, Avoiding interpolation artifacts in Stolt migration: SEP-30, 103-110.
- Krebes, E.S., 2006, Seismic theory and methods: Course notes.
- Lin, J., Teng, L. and Muir, F., 1997, Comparison of different interpolation methods for Stolt migration: http://sepwww.stanford.edu/public/docs/sep79/intime5/paper_html/index.html, accessed March 26, 2007.
- Margrave, G.F., 2003, CREWES educational software and data release (MATLAB): <http://www.crewes.org/Samples/EduSoftware/ReleaseAgreement.html>, accessed March 26, 2007.
- Margrave, G.F., 2007, Methods of seismic data processing: course notes.
- Popovici, A.M., Blondel, P., and Muir, F., 1997, Interpolation in Stole migration: SEP-79, 275-282.
- Rosenbaum, J.H. and Boudreaux, G.F., 1981, Rapid convergence of some seismic processing algorithms: *Geophysics*, **46**, 1667-1672.